NANO LETTERS

Letter

pubs.acs.org/NanoLett

Biocompatible Label-Free Detection of Carbon Black Particles by Femtosecond Pulsed Laser Microscopy

Hannelore Bové,[†,‡] Christian Steuwe,[‡] Eduard Fron,[§] Eli Slenders,[†] Jan D'Haen,[∥] Yasuhiko Fujita,[§] Hiroshi Uji-i,[§,⊥] Martin vandeVen,[†] Maarten Roeffaers,*[,‡] and Marcel Ameloot*[,†]

[†]Biomedical Research Institute, Hasselt University, Agoralaan Building C, 3590 Diepenbeek, Belgium

[‡]Centre for Surface Chemistry and Catalysis and [§]Department of Chemistry, KU Leuven, Celestijnenlaan 200F, 3001 Leuven, Belgium

[∥]Institute for Material Research, Hasselt University, Wetenschapspark 1, 3950 Diepenbeek, Belgium

[⊥]Research Institute for Electronic Science, Hokkaido University, N20W10, Kita-Ward Sapporo 001-0020, Japan

Supporting Information

ABSTRACT: Although adverse health effects of carbon black (CB) exposure are generally accepted, a direct, label-free approach for detecting CB particles in fluids and at the cellular level is still lacking. Here, we report nonincandescence related white-light (WL) generation by dry and suspended carbon black particles under illumination with femtosecond (fs) pulsed near-infrared light as a powerful tool for the detection of these carbonaceous materials. This observation is done for four different CB species with diameters ranging from 13 to 500 nm, suggesting this WL emission under fs near-infrared illumination is a general property of CB particles. As the emitted radiation spreads over the whole visible spectrum, detection is straightforward and flexible. The unique property of the described WL emission allows optical detection and unequivocal localization of CB particles in fluids and in cellular environments while simultaneously colocalizing different cellular components using various specific fluorophores as shown here using human lung fibroblasts. The experiments are performed on a typical multiphoton laser-scanning microscopy platform, widely available in research laboratories.

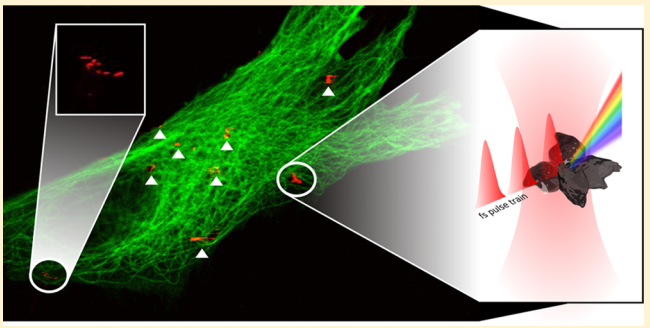

KEYWORDS: *Carbon black particles, label-free detection in aqueous environments, white light emission, femtosecond pulsed laser illumination, human lung fibroblasts*

Carbon black (CB) consists of aciniform aggregates of primary particles with an elemental carbon content greater than 97%.[1,2] It is produced through well-controlled incomplete combustion of organics like heavy petroleum or vegetable oil. This distinguishes CB from soot or black carbon, the unwanted byproduct released during incomplete combustion processes such as in the exhausts of diesel engines and one of the main contributing factors to atmospheric particulate pollution.[2,3] Nonetheless, due to the (physico)chemical similarity CB is widely used as a model compound for soot.[4,5] The total global black carbon emission was estimated to be approximately 8.5 million tons after having constantly increased throughout the preceding decade.[6−8] As a consequence of the increasing environmental and occupational exposure to these carbonaceous particles, deeper insight into the (eco-) toxicological impact of these materials is of critical importance.

So far, however, no experimental methods have been reported that enable direct detection of carbon black/black carbon in relevant samples such as polluted water and consumer products as well as exposed cells and body fluids. To date, only measurements[9−11] in polluted air (see ref 9 for an overview) such as absorption photometry and laser-induced incandescence (LII) have been used to determine particle concentrations or alternatively labeling methods[12−14] have been explored such as the technetium-99-m radionuclide labeling in epidemiological studies and toxicology research.

In LII, the emission from carbonaceous materials has been linked to blackbody radiation from the severely heated CB particles,[15] that is, incandescence. Already various models have been proposed to explain the origin of incandescence and its dependence on illumination power and pulse duration.[16−18] Recently, substantial scientific efforts have focused on white light (WL) emission from carbonaceous materials including graphene,[19] fullerenes,[20] and carbon nanotubes.[21] Also for these materials the emitted radiation has been linked to incandescence. However, visible emission from CB particles in solution and biological matter has so far not been sufficiently explored,

Received: February 4, 2016
Revised: April 16, 2016
Published: April 22, 2016

DOI: 10.1021/acs.nanolett.6b00502
Nano Lett. 2016, 16, 3173−3178

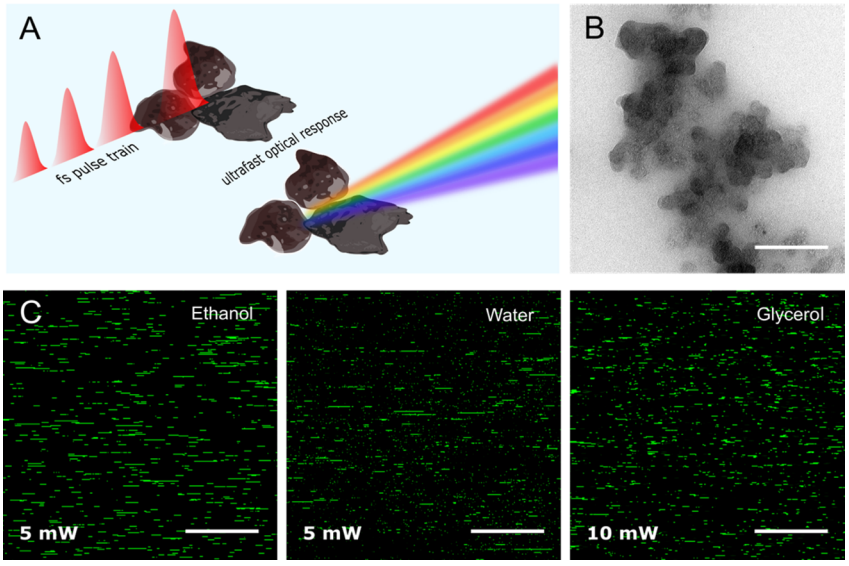

Figure 1. (A) Schematic representation of the illumination and emission process of CB particles for the presented detection method. (B) TEM image of an ufPL aggregate. Scale bar: 300 nm. (C) CCB (600 μg/mL) imaging in ultrapure water, ethanol, and glycerol at room temperature upon illumination with 5 or 10 mW average laser power at the sample (excitation 810 nm, 80 MHz). Scale bars: 15 μm. Emission band: 450−650 nm.

despite reports of CB suspensions serving as optical limiters and nonlinear scatterers due to their broadband and flat absorption.[16,17] The interpretation of these effects is not straightforward as they strongly depend on the experimental conditions.[22] Recently, luminescence of carbon particles has been described but this phenomenon seems to be limited to carbon nanodots, that is, carbon nanoparticles with sizes below 10 nm.[23,24]

To the best of our knowledge, we report here for the first time nonincandescence related WL emission of CB particles in aqueous environments under femtosecond pulsed illumination using a multiphoton laser-scanning microscope and demonstrate its potential in a biological context. This label-free approach to directly visualize CB offers additional advantages (schematic representation in Figure 1A) such as inherent 3D sectioning and high imaging depths owing to the multiphoton approach. We anticipate that this method will play an important role in health-related studies where the impact and role of CB particles is to be assessed at the organism, tissue, cellular, and subcellular level.

In this study, a variety of carbonaceous particles, representative for those to which humans are typically exposed, is used ranging from powders used in copy machines to materials that are typically employed as model for soot. Information on the physicochemical characteristics of these different commercial CB materials (ufPL, ufP90, CCB, and fCB) can be found in Table S1 in the Supporting Information (SI). According to manufacturer's data, the aerodynamic diameter of the particles varies between 13 and 500 nm. Transmission electron microscopy (TEM) images (Figures 1B and S1) show the typical appearance of CB consisting of aciniform aggregates of primary carbon particles with arbitrary shape. These TEM images and the results from dynamic light scattering summarized in Table S1 show that CB particles aggregate when suspended in aqueous solutions, and absorb corona proteins from the complete medium onto their surface resulting in an increased hydrodynamic diameter and a zeta-potential corresponding to approximately −20 mV regardless of their native potential. In conclusion, the physicochemical characteristics of the different CB particles in suspension are similar although when selecting the particles we aimed for as much difference as possible.

Figure 1C displays CB suspended in ultrapure water, ethanol, and glycerol illuminated with a femtosecond laser at 810 nm (150 fs, 80 MHz) and recorded using a commercial multiphoton laser-scanning microscope (detailed information on sample preparation and microscopy modalities can be found in SI). Intense signals were detected with an emission band-pass filter of 450 to 650 nm in front of the detector. Depending on the suspension medium, the laser power needs to be adjusted to generate similar emission intensity; in glycerol and immersion oil, the illumination power was about twice that of the experiment in ethanol or water (SI, Figure S2). Note the horizontal smearing of the CB particles in Figure 1C (pixel dwell time of 1.60 μs, pixel size of 220 nm). This phenomenon is observed at all combinations of scan speeds and zooms (data not shown), suggesting susceptibility of the particles to optical trapping under these conditions. This hypothesis is further supported by the absence of this smearing when CB particles are embedded in polydimethylsiloxane (Figure S3). Trapping by femtosecond laser pulses has already been shown for other types of nanoparticles.[25,26]

Additional spectroscopic measurements were performed to investigate the observed visible light emission under femtosecond near-infrared illumination.

First, we rule out photoluminescence (PL) reported for very small carbonaceous particles (below 10 nm)[23,24,27] as a cause of the observed emission. Carbonaceous particles, in particular soot, consist of aggregated particles that are heterogeneous in nature[28] and therefore contain multiple absorbing species possibly responsible for radiative transitions. The extinction spectra of aqueous suspensions of the CB particles considered here cover the whole visible range (Figure 2A), presumably due to a continuum of electronic states in the amorphous carbon. The slight increase of the extinction toward lower wavelengths for the two smaller particles (ufPL and ufP90) is likely due to increased light scattering.

DOI: 10.1021/acs.nanolett.6b00502
Nano Lett. 2016, 16, 3173−3178

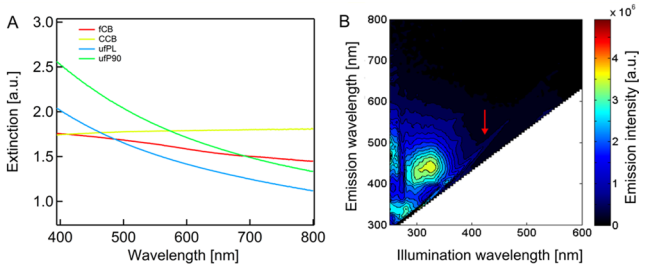

Figure 2. (A) Extinction spectra of aqueous CB suspensions. (B) Two-dimensional excitation−emission plot of ufPL particles in water under single photon excitation with a false color map based on the emission intensity in arbitrary units. The red arrow points toward the Raman line of water.

Two-dimensional single photon excitation−emission plots (Figure 2B) of ufPL (similar plot for fCB: SI, Figure S4) however, show only weak emission; note in comparison the weak Raman line (red arrow) of water, the suspension medium. The luminescence under excitation in the ultraviolet (UV) region (280−380 nm) looks similar to the observations described by Kwon et al. for carbon nanodots[29,30] and hints toward microcrystalline graphite exhibiting only a low number of tetrahedral sp^3-sites[30−32] which is also confirmed by Raman spectra (SI, Figure S5).

In contrast to single photon excitation, illumination with femtosecond pulsed near-infrared light (810 nm, 150 fs, 80 MHz) generates a strong, feature-less white light emission stretching the whole visible spectrum (Figure 3A,B). This observation was made for all four types of aqueous CB suspensions used in this study and even for dry particles (SI, Figure S6). This WL emission is independent of the illumination wavelength within the range of 780 to 900 nm for a constant average power of 8 mW at the sample (Figure 3B, see also SI, Figure S7).

While PL as visible in Figure 2B cannot explain the strong WL emission observed under femtosecond illumination (Figures 1C, 3A,B), time-resolved investigations are indicative. Using time correlated single photon equipment, an instantaneous nature of the WL radiation is noticed when looking at the picosecond time scale (SI, Figure S8). Also, in femtosecond up-conversion experiments with a higher temporal resolution the emitted signal of the CB particles is witnessed to be instantaneous (Figure 3C). On further note, illumination with 7 ps pulses results in a strongly reduced luminescence intensity (SI, Figure S9). The WL emission from the suspended CB particles is therefore only efficiently triggered by femtosecond illumination with high peak electromagnetic fields and once the femtosecond illumination pulse ceases, the WL emission terminates immediately.

The instantaneous nature of the observed signal confirms that we are not dealing with incandescence despite using laser illumination with fluences of about 0.05 J/cm^2 at 0.1 nJ pulse energy, similar to previous experiments. In those reports, the observed incandescence showed clear decay times in the microsecond time scale regime[31] due to the cooling down of the lattice at these time scales. In fact, heating of the particle lattice, which is required for incandescence, only occurs on a picosecond time scale when remaining nonemitted energy will be converted into lattice vibrations.[32−34] The femtosecond illumination employed here is too fast.

The observed instantaneous WL emission is also not related to local refractive index changes in the CB nanoparticle environment upon pulse arrival. Gold nanoparticles, for example, are known to form nanometer-sized bubbles when illuminated with pulsed lasers at laser fluencies similar to those applied here[31,35] and those have been observed leading to broad featureless WL emission.[35−38] If a related principle would be underlying the observed WL emission in CB suspension, the emission spectra would be strongly influenced by the surrounding refractive index. However, even dry particles show the same spectral profile as those suspended in water (SI, Figure S6).

We believe that the observed visible light emission under femtosecond near-infrared illumination is related to the broad anti-Stokes emission with nonlinear power dependence that was previously observed by other groups for noble metal nanoparticles. In those experiments, the emission arose from femtosecond illumination of gold and silver particles or nanostructures.[39−42] We can confirm that also the WL emission of CB displays a nonlinear, second order response with respect to the incident power (SI, Figure S10). The WL emission of gold was recently succinctly investigated by Haug et al.[43] Here, plasmonic confinement of electric fields in metal along with the small dimensions of the emitting particle can presumably relax symmetry selection and momentum conservation rules to allow for (continuous) intraband dipole transitions, which would otherwise be impossible. The observed emission is independent of the type of metal and the preparation conditions. Even though carbon particles are not metallic in nature and do not show plasmonic modes in the visible or near UV spectral range (see Figure 2A), an electron gas could emerge on arrival of a femtosecond pulse. At very high energies, even plasmons or

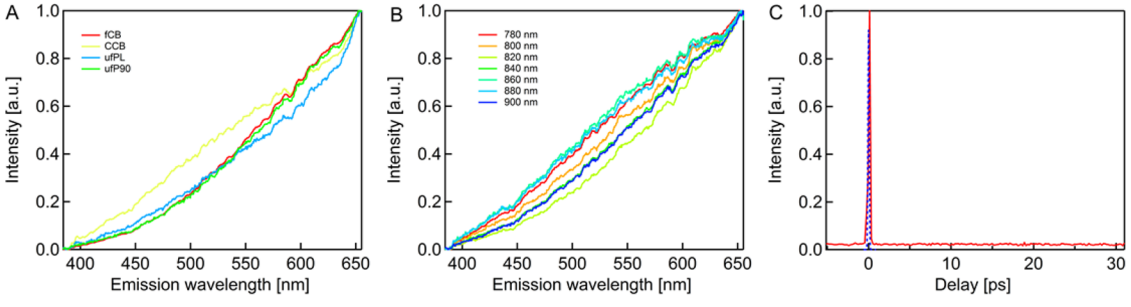

Figure 3. (A) Normalized WL emission spectra of aqueous CB particle suspensions using femtosecond 810 nm laser illumination (8 mW, 150 fs, 80 MHz). (B) Normalized WL emission spectra of aqueous ufP90 suspensions recorded at different femtosecond illumination wavelengths. (C) Temporal response of aqueous carbon suspension measured by femtosecond photoluminescence up-conversion experiments. Also shown is the instrument response function (dashed line).

DOI: 10.1021/acs.nanolett.6b00502
Nano Lett. 2016, 16, 3173−3178

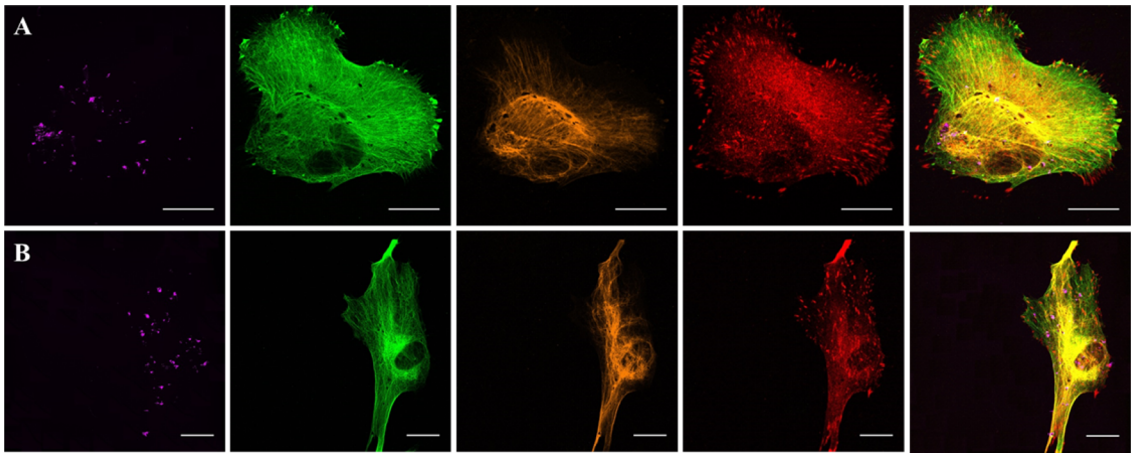

Figure 4. Imaging of cellular compartments of fixed MRC-5 cells stained with commonly utilized fluorophores and in combination with the detection of CCB particles (4 h incubation of 5 $\mu g/cm^2$ CCB at 37 °C prior to imaging). Emission of the carbonaceous particles can be probed at different wavelengths, here shown at (A) 400−410 nm in the nondescanned mode and (B) 650−710 nm in descanned mode (4 mW average laser power at the stage). From left to right: CCB particles, tubulin cytoskeleton (Ex/Em 495/519 nm, ∼3 μW radiant power at the sample), vimentin, which is an intermediate filament protein of the cytoskeleton (Ex/Em 555/565 nm, ∼3 μW radiant power at the sample), paxillin expressed at focal adhesions (Ex/Em 650/665 nm, ∼3 μW radiant power at the sample), and overlay image. Scale bars: 25 μm.

plasmon-like effects have been discovered with electron energy loss spectroscopy in carbon nanotubes and its parent material graphene[44−46] or in graphitic spheres.[47] Buckminsterfullerene[48] and other carbonaceous materials[49] show strong multiphoton ionization. The intense and spectrally broad absorption of the particles could give rise to this phenomenon, promoting resonant multiphoton transitions leading to ionizations.[50] Therefore, consecutive intraband transitions similar to those noticed in plasmonically active metals could be a valid explanation for the observed results.

As a result of visible WL generation by carbon black particles under femtosecond pulsed near-infrared illumination, the signal of the particles can easily be combined with various conventional contrast-enhancing fluorophores used to visualize biological features. As shown in Figure 4, the emitted WL can be probed at different wavelengths at laser powers compatible with life cell imaging. Hence, CB detection can be combined with the imaging of cellular compartments stained by different color-label fluorophores (labeling strategy can be found in SI). This simultaneous detection enables unequivocally localization of the particles inside the cells and puts the CB location directly into its biological context.

To further illustrate the versatility of the technique in a biological setting, a colocalization study of the tubulin cytoskeleton of MRC-5 lung fibroblasts and engulfed carbon particles was performed (Figure 5). The images show a clear impact of CCB on the architecture of the tubulin cytoskeleton of the cells for an incubation that exceeds 4 h at 37 °C. More specifically, the supporting cytoskeleton network evolves from the commonly observed fiberlike structure to a partial diffuse and holey configuration. The cytoskeletal alteration is also reflected in the overall morphology of the cells. Their appearance changed from the normal bipolar and stretched morphology to a smaller and more irregular-shaped one, which is an indication of apoptosis (these biological findings are also true for the other smaller CB particles, for an additional example with ufP90, see SI, Figure S11).[51−53] These images do not only pinpoint the versatility in biological settings but also immediately indicate the social relevance and significance of this detection technique. Potential advantageous information

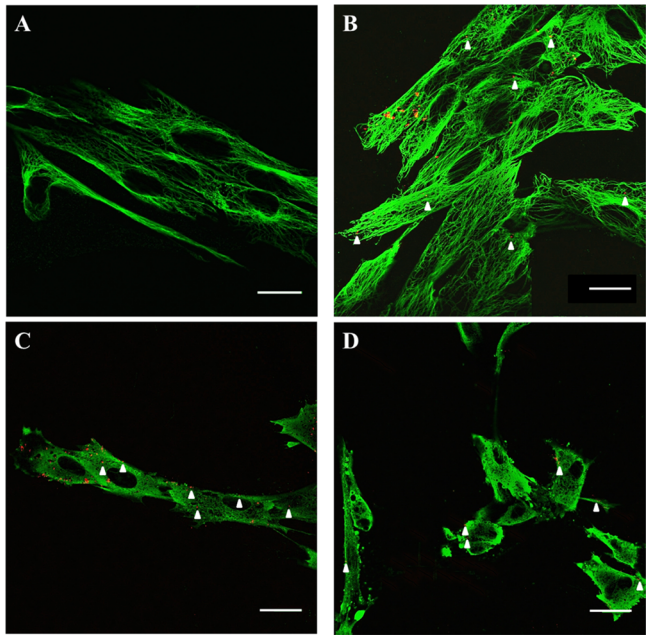

Figure 5. Tubulin cytoskeleton (green, Ex/Em 495/519 nm, ∼3 μW radiant power at the sample) of normal human lung fibroblasts incubated with 5 $\mu g/cm^2$ CCB particles (red, 4 mW average laser power at the sample, emission detection, 400−410 nm in non-descanned mode) at 37 °C. (A) Control cells; (B) 4 h incubation; (C) 8 h incubation; (D) 24 h incubation. Scale bars: 30 μm. Arrow heads, some locations of very small, engulfed CCB particles.

arising from this simultaneous detection comprises the correlations that can be made between the location of the particles and the altered cellular structure (e.g., cytoskeleton and focal adhesions). This makes the observed WL emission an extremely interesting label-free detection mechanism for biomedical research including toxicology and epidemiology.

To conclude, femtosecond pulsed illumination of CB followed by detection of emitted WL is a straightforward approach without the need of particular sample pretreatment and which can easily be implemented in multiphoton imaging

DOI: 10.1021/acs.nanolett.6b00502
Nano Lett. 2016, 16, 3173−3178

experiments. The nature of the signal makes it very versatile in terms of choice of additional fluorophores. The ease of the reported approach broadens the potential applicability in the fast growing field of nanotechnology. Additionally, it will advance epidemiological and toxicological studies because this is the first time a technique is described to directly detect carbon black in a biological setting without any additional treatment or labeling required. We anticipate that this technology will make it possible to screen human tissues and body fluids for the presence of CB owing to the multiphoton approach that results in inherent 3D sectioning and high imaging depths. This may eventually lead to valuable information about, for example, the actual uptake and clearance of CB particles by the human body.

■ ASSOCIATED CONTENT

Supporting Information

The Supporting Information is available free of charge on the ACS Publications website at DOI: 10.1021/acs.nanolett.6b00502.

Detailed methods and supplemental figures. (PDF)

■ AUTHOR INFORMATION

Corresponding Authors

*(M.R.) E-mail: maarten.roeffaers@biw.kuleuven.be. Phone: +3216-327-449.

*(M.A.) E-mail: marcel.ameloot@uhasselt.be. Phone: +3211-269-233.

Author Contributions

H.B. and C.S. contributed equally to this work. H.B., C.S., M.R., and M.A. jointly designed and analyzed the experiments. H.B. and C.S. performed most of the experiments. E.F. performed the femtosecond fluorescence up-conversion experiments. E.S. assisted with the time-correlated single photon counting. J.D. made the transmission electron microscopy images. H.U. and Y.F. gave their technical support during spectral data collection. M.V. gave theoretical support. The manuscript was written through contributions of all authors. All authors have given approval to the final version of the manuscript.

Notes

The authors declare no competing financial interests.

■ ACKNOWLEDGMENTS

This research was supported by the Interuniversity Attraction Poles Program (P7/05) initiated by the Belgian Science Policy Office. H.B. acknowledges funding from Research Foundation Flanders (Fonds Wetenschappelijk Onderzoek, FWO) for a doctoral Fellowship: 11ZB115N. C.S. is supported by a postdoctoral FWO fellowship: 12R6315N. The authors also thank FWO for the research Grant G082113. M.R. acknowledges financial support from the KU Leuven Research Fund (C14/15/053, OT/12/059). M.A. thanks the Province of Limburg (Belgium) for the financial support within the tUL IMPULS FASE II program, allowing for the upgrading of the laser source used in this work. W. Baekeland is acknowledged for his support with the recording of the single photon extinction and emission spectra. H.B. gratefully acknowledges the assistance of Mrs. P. Bex and Mr. J. Janssen.

■ REFERENCES

(1) ASTM, American Society for Testing Materials D3053-13a; *Standard on Terminology Relating to Carbon Black*; ASTM International: West Conshohocken, PA, 2013.

(2) Watson, A. Y.; Valberg, P. A. *AIHAJ* **2001**, *62* (2), 218−228.

(3) Castro, L.; Pio, C.; Harrison, R. M.; Smith, D. *Atmos. Environ.* **1999**, *33* (17), 2771−2781.

(4) Arnal, C.; Alzueta, M.; Millera, A.; Bilbao, R. *Combust. Sci. Technol.* **2012**, *184* (7−8), 1191−1206.

(5) Tankersley, C. G.; Bierman, A.; Rabold, R. *Inhalation Toxicol.* **2007**, *19* (8), 621−9.

(6) Bond, T. C.; Bhardwaj, E.; Dong, R.; Jogani, R.; Jung, S.; Roden, C.; Streets, D. G.; Trautmann, N. M. *Glob. Biogeochem. Cycles* 2007, *21* (2), 1−16.

(7) Lamarque, J.-F.; Bond, T. C.; Eyring, V.; Granier, C.; Heil, A.; Klimont, Z.; Lee, D.; Liousse, C.; Mieville, A.; Owen, B. *Atmos. Chem. Phys.* **2010**, *10* (15), 7017−7039.

(8) Wang, R. *Global Emission Inventory and Atmospheric Transport of Black Carbon: Evaluation of the Associated Exposure*; Springer Theses: Beijing, China, 2015.

(9) Chow, J. C.; Watson, J. G.; Doraiswamy, P.; Chen, L.-W. A.; Sodeman, D. A.; Lowenthal, D. H.; Park, K.; Arnott, W. P.; Motallebi, N. *Atmos. Res.* **2009**, *93* (4), 874−887.

(10) OECD. *Methods of Measuring Air Pollution: Report of the Working Party on Methods of Measuring Air Pollution and Survey Techniques*; Organization for Economic Co-operation and Development: Paris, France, 1964.

(11) Schulz, C.; Kock, B. F.; Hofmann, M.; Michelsen, H.; Will, S.; Bougie, B.; Suntz, R.; Smallwood, G. *Appl. Phys. B: Lasers Opt.* **2006**, *83* (3), 333−354.

(12) Kong, H.; Zhang, Y.; Li, Y.; Cui, Z.; Xia, K.; Sun, Y.; Zhao, Q.; Zhu, Y. *Int. J. Mol. Sci.* **2013**, *14* (11), 22529−22543.

(13) Wang, H.-f.; Troxler, T.; Yeh, A.-g.; Dai, H.-l. *J. Phys. Chem. C* **2007**, *111* (25), 8708−8715.

(14) Nemmar, A.; Hoet, P. M.; Vanquickenborne, B.; Dinsdale, D.; Thomeer, M.; Hoylaerts, M.; Vanbilloen, H.; Mortelmans, L.; Nemery, B. *Circulation* **2002**, *105* (4), 411−414.

(15) Ferrari, A.; Meyer, J.; Scardaci, V.; Casiraghi, C.; Lazzeri, M.; Mauri, F.; Piscanec, S.; Jiang, D.; Novoselov, K.; Roth, S. *Phys. Rev. Lett.* **2006**, *97* (18), 187401.

(16) Belousova, I.; Mironova, N.; Scobelev, A.; Yur'ev, M. *Opt. Commun.* **2004**, *235* (4), 445−452.

(17) Zelensky, S. *Semicond. Phys. Quantum Electron. Optoelectron.* **2004**, *7* (2), 190−194.

(18) Rulik, J. J.; Mikhailenko, N.; Zelensky, S.; Kolesnik, A. *Semicond. Phys. Quantum Electron. Optoelectron.* **2007**, *10* (2), 6−10.

(19) Strek, W.; Cichy, B.; Radosinski, L.; Gluchowski, P.; Marciniak, L.; Lukaszewicz, M.; Hreniak, D. *Light: Sci. Appl.* **2015**, *4* (1), e237.

(20) Hamilton, B.; Rimmer, J.; Anderson, M.; Leigh, D. *Adv. Mater.* **1993**, *5* (7−8), 583−585.

(21) Imholt, T.; Dyke, C. A.; Hasslacher, B.; Pérez, J. M.; Price, D.; Roberts, J. A.; Scott, J.; Wadhawan, A.; Ye, Z.; Tour, J. M. *Chem. Mater.* **2003**, *15* (21), 3969−3970.

(22) Fougeanet, F.; Fabre, J.-C. In *Nonlinear mechanisms in carbon-black suspension in a limiting geometry*; MRS Proceedings; Cambridge University Press: New York, 1997; p 293.

(23) Li, H.; Kang, Z.; Liu, Y.; Lee, S.-T. *J. Mater. Chem.* **2012**, *22* (46), 24230−24253.

(24) Ghosh, S.; Chizhik, A. M.; Karedla, N.; Dekaliuk, M. O.; Gregor, I.; Schuhmann, H.; Seibt, M.; Bodensiek, K.; Schaap, I. A.; Schulz, O. *Nano Lett.* **2014**, *14* (10), 5656−5661.

(25) Usman, A.; Chiang, W. Y.; Masuhara, H. *Sci. Prog.* **2013**, *96* (1), 1−18.

(26) Usman, A.; Chiang, W.-Y.; Masuhara, H. *Proc. SPIE* **2012**, 845833−845833−7.

(27) Li, Q.; Ohulchanskyy, T. Y.; Liu, R.; Koynov, K.; Wu, D.; Best, A.; Kumar, R.; Bonoiu, A.; Prasad, P. N. *J. Phys. Chem. C* **2010**, *114* (28), 12062−12068.

DOI: 10.1021/acs.nanolett.6b00502
Nano Lett. 2016, 16, 3173−3178

(28) Bond, T. C.; Bergstrom, R. W. *Aerosol Sci. Technol.* **2006**, *40* (1), 27−67.
(29) Kwon, W.; Do, S.; Kim, J.-H.; Jeong, M. S.; Rhee, S.-W. *Sci. Rep.* **2015**, *5*, 12604.
(30) Carpene, E.; Mancini, E.; Dallera, C.; Schwen, D.; Ronning, C.; De Silvestri, S. *New J. Phys.* **2007**, *9* (11), 404.
(31) Michelsen, H. A. *J. Chem. Phys.* **2003**, *118* (15), 7012−7045.
(32) Link, S.; El-Sayed, M. A. *J. Phys. Chem. B* **1999**, *103* (40), 8410−8426.
(33) Ahmadi, T. S.; Logunov, S. L.; El-Sayed, M. A. *J. Phys. Chem.* **1996**, *100* (20), 8053−8056.
(34) Hodak, J.; Martini, I.; Hartland, G. V. *Chem. Phys. Lett.* **1998**, *284* (1), 135−141.
(35) Kotaidis, V.; Dahmen, C.; Von Plessen, G.; Springer, F.; Plech, A. *J. Chem. Phys.* **2006**, *124* (18), 184702.
(36) Lapotko, D. *Opt. Express* **2009**, *17* (4), 2538−2556.
(37) Lapotko, D. *Int. J. Heat Mass Transfer* **2009**, *52* (5), 1540−1543.
(38) Lukianova-Hleb, E. Y.; Sassaroli, E.; Jones, A.; Lapotko, D. O. *Langmuir* **2012**, *28* (10), 4858−4866.
(39) Kim, H.; Sheps, T.; Taggart, D. K.; Collins, P. G.; Penner, R. M.; Potma, E. O. In *Coherent anti-Stokes generation from single nanostructures*; Proc. SPIE 7183; Multiphoton Microscopy in the Biomedical Sciences IX: San Jose, CA, 2009; pp 718312−718312-8.
(40) Beversluis, M. R.; Bouhelier, A.; Novotny, L. *Phys. Rev. B: Condens. Matter Mater. Phys.* **2003**, *68* (11), 115433.
(41) Danckwerts, M.; Novotny, L. *Phys. Rev. Lett.* **2007**, *98* (2), 026104.
(42) Palomba, S.; Danckwerts, M.; Novotny, L. *J. Opt. A: Pure Appl. Opt.* **2009**, *11* (11), 114030.
(43) Haug, T.; Klemm, P.; Bange, S.; Lupton, J. M. *Phys. Rev. Lett.* **2015**, *115* (6), 067403.
(44) Kramberger, C.; Hambach, R.; Giorgetti, C.; Rümmeli, M.; Knupfer, M.; Fink, J.; Büchner, B.; Reining, L.; Einarsson, E.; Maruyama, S. *Phys. Rev. Lett.* **2008**, *100* (19), 196803.
(45) Ajayan, P.; Iijima, S.; Ichihashi, T. *Phys. Rev. B: Condens. Matter Mater. Phys.* **1993**, *47* (11), 6859.
(46) Pichler, T.; Knupfer, M.; Golden, M.; Fink, J.; Rinzler, A.; Smalley, R. *Phys. Rev. Lett.* **1998**, *80* (21), 4729.
(47) Stöckli, T.; Bonard, J.-M.; Châtelain, A.; Wang, Z. L.; Stadelmann, P. *Phys. Rev. B: Condens. Matter Mater. Phys.* **1998**, *57* (24), 15599.
(48) Ding, D.; Compton, R.; Haufler, R.; Klots, C. *J. Phys. Chem.* **1993**, *97* (11), 2500−2504.
(49) Pratt, S. T.; Dehmer, J. L.; Dehmer, P. M. *J. Chem. Phys.* **1985**, *82* (2), 676−680.
(50) Streibel, T.; Zimmermann, R. *Annu. Rev. Anal. Chem.* **2014**, *7*, 361−381.
(51) Hussain, S.; Thomassen, L. C.; Ferecatu, I.; Borot, M.-C.; Andreau, K.; Martens, J. A.; Fleury, J.; Baeza-Squiban, A.; Marano, F.; Boland, S. *Part. Fibre Toxicol.* **2010**, *7* (1), 10.
(52) Sydlik, U.; Bierhals, K.; Soufi, M.; Abel, J.; Schins, R. P.; Unfried, K. *Am. J. Physiol. Lung Cell. Mol. Physiol.* **2006**, *291* (4), L725−L733.
(53) Bortner, C.; Cidlowski, J. *Cell Death Differ.* **2002**, *9* (12), 1307−1310.

DOI: 10.1021/acs.nanolett.6b00502
Nano Lett. 2016, 16, 3173−3178